# Granular Cu-Co alloys as interacting superparamagnets

Paolo Allia,[1] Marco Coisson,[2] Paola Tiberto,[3] Franco Vinai,[3] Marcelo Knobel,[4] M. A. Novak,[5] and W. C. Nunes[5]
[1]*Dipartimento di Fisica, Politecnico di Torino, I-10129 Torino, Italy and INFM, UdR TO-Poli, I-10129 Torino, Italy*
[2]*DISPEA, Politecnico di Torino, I-10129 Torino, Italy and INFM, UdR TO-Poli, I-10129 Torino, Italy*
[3]*IEN Galileo Ferraris, I-10125 Torino, Italy, and INFM, UdR TO-Poli, I-10129 Torino, Italy*
[4]*Instituto de Fisica Gleb Wataghin, UNICAMP, C.P. 6165, 13083-970, Campinas, S.P., Brazil*
[5] *Instituto de Fisica, UFRJ, 21945-970 Rio de Janeiro, Brazil*
(Received 5 April 2001; published 20 September 2001)

The anhysteretic magnetization of the granular metallic alloy $Cu_{90}Co_{10}$ is experimentally studied over a wide temperature range (2–700 K). The measurements definitely exclude that this alloy is a simple superparamagnet, even in the high-temperature limit, although some features of granular systems [such as the typical Langevin-like form of the anhysteretic magnetization curves $M(H)$] are often taken as evidence of superparamagnetism. A phenomenological theory is proposed, explicitly considering that particle moments interact through long-ranged dipolar random forces, whose effect is pictured in terms of a temperature $T^*$, adding to the actual temperature $T$ in the denominator of the Langevin function argument. This simple formula explains all features of the experimental $M(H)$ curves. The theory indicates that the actual magnetic moments on interacting Co particles are systematically larger than those obtained fitting the magnetic data to a conventional Langevin function. The $Cu_{90}Co_{10}$ granular alloy is therefore identified as an ''interacting superparamagnet'' ISP. The ISP regime appears as separating the high-temperature, conventional superparamagnetic phase from the low-temperature, blocked-particle regime. In this way, a magnetic-regime diagram can be drawn for each granular system. The competition between single-particle and collective blocking mechanisms is briefly analyzed. The proposed interpretation is thought to be applicable to other fine particle systems; its main features and intrinsic limits are discussed.

DOI: 10.1103/PhysRevB.64.144420 PACS number(s): 75.20.−g, 75.50.Tt, 75.75.+a

## I. INTRODUCTION

Although the magnetism of fine particles has been studied for almost 55 years, it is amazing to note the rich variety of phenomena which remain to be understood in nanoscale granular systems.[1] A complete understanding of the magnetic properties of nanoscopic systems is hindered by their inherent complexity, involving broad particle size distributions, different structural and/or magnetic phases, local anisotropies, and interparticle magnetic interactions.[2] In fact, it is extremely difficult to properly understand which factor plays a dominant role in the magnetic behavior of granular systems in order to achieve a better knowledge of their fundamental properties and possibly optimize them for prospective technological applications.

As an example, let us consider a basic aspect of any magnetic material, i.e., its isothermal magnetization curve. In particular, we shall focus here on a specific type of granular solid, melt-spun Cu-Co ribbons, but the basic ideas can in principle be applied to any granular system. At room temperature these samples display isothermal magnetization curves exhibiting a superparamagnetic behavior, as indeed expected, but with a definite if slight hysteresis, with coercive fields around 100–400 Oe. Several investigations indicate that the system consists of nanometric grains (with diameters typically below 8 nm), distributed in sizes following approximately a log-normal distribution.[3] However, although Cu-Co ribbons have been extremely well characterized in the last years (mainly owing to their magnetoresistance properties[4]), several questions remain open or only partially addressed, regarding (i) the Langevin-like behavior of the experimental anhysteretic curves, (ii) the lack of agreement between the experimental data and the well-established superparamagnetic picture,[5] and (iii) the physical origin of the hysteresis observed up to high temperatures (few particles in the blocked regime versus magnetic interactions among Co particles). Recently, the last point was investigated in some detail: a theoretical approach has been proposed in order to take into account the role of magnetic interactions among particles.[6] Essentially, the theory makes use of a mean-field approach, where a memory function related to an effective interaction field $H_0$ emerges as responsible for the observed hysteresis. In spite of the complexity of the system, the model admits analytic solutions in the case of pure dipolar interactions and can be easily applied to granular magnetic systems. However, many nonmarginal problems related to the anysteretic experimental curves [points (i) and (ii)] are still to be solved, as will be explained in further detail in Sec. III.

A large number of experimental papers containing a variety of results have been published in the last years.[7–15] Furthermore, computer simulations have extensively been used, leading to several contradictory conclusions, mainly dependent on the approach adopted to investigate the problem. Several recent works have found important deviations from the classical Langevin law in the case of pure superparamagnetic systems and usually attribute the deviations to the presence of strong anisotropies, also mentioning the possible existence of magnetic interactions.[16–18] Regarding the problem of magnetic interactions, many different—and often conflicting—models have been applied to explain the experi-

 

mental data. One of the approaches considers the interparticle interactions as merely changing the energy barriers of isolated particles.[19] This approach corresponds to replacing a genuine many-body effect by a single-particle description; it is therefore no more than a simplified representation of a much more complex, qualitatively different situation. On the other hand, a second approach takes into account collective phenomena,[20] but the predictions of such a model seem to contradict many experimental results. Consequently, there has been a considerable discussion about the existence of significant collective effects in magnetic nanoparticle systems and several speculations regarding a spin-glass-like phase at low temperatures on dipole-dipole interacting systems.[21]

Often, the results of magnetization-curve measurements on granular systems are exploited as a quick, inexpensive tool to get first hand information about the average particle size and possibly about the particle-size distribution. To this aim, the experimental curves are usually fitted to a superposition of properly weighted Langevin curves, differing by their argument; the magnetic moments on particles are thus easily determined, and the particle size is finally obtained, making some further assumptions about the local magnetic coherence of the spins in a particle and about the shape of the particles.

In many systems, such as Cu-Co granular ribbons, the experimental magnetization curves are remarkably well fitted by Langevin functions at any given temperature. However, the agreement may be misleading. In this work, we definitely show that the classical superparamagnetic model fails to coherently account for the results of a systematic study of isothermal magnetization curves measured at different temperatures. To our knowledge, no attempt to reconcile these incoherent results using a single unifying concept has been proposed so far.

The experimental evidence of a systematic discrepancy between the predictions of the superparamagnetic model and the experimental data leads us to assume that the role of magnetic interactions is more substantial than usually considered. The problem of how to represent such a collective effect is solved by introducing a proper transformation in the argument of the Langevin function. In this way, a different magnetic regime, referred to as the ''interacting superparamagnet,'' is defined and applied to the particular case of $Cu_{90}Co_{10}$ granular ribbons. The isothermal magnetization curves measured in these systems over a wide temperature range (2–700 K) turn out to be coherently described in a remarkably simple way by a single formula.

## II. EXPERIMENT

Continuous ribbons of nominal composition $Cu_{90}Co_{10}$ were produced by melt spinning in Ar atmosphere using a Cu-Zr drum. The preparation technique was previously exploited to obtain $Cu_{100-x}Co_x$ ribbons with $x=3-30$.[22] Many different $Cu_{90}Co_{10}$ samples were prepared, using slightly different preparation parameters and submitting the as-quenched materials to different thermal treatments (both in furnace and by Joule heating in vacuum[23]), in order to modify the nanostructure of the material and obtain different magnetic and transport properties.[6,22] A summary of preparation parameters and pretreatments for all studied samples is given in Table I.

The magnetization curves of samples 1 and 2 were measured in Torino at different temperatures [from room temperature (RT) up to 900 K] using a vibrating sample magnetometer (LDJ model 9600), with a maximum field of 10 kOe. The isothermal magnetization curves of samples 3–5 were measured in Rio de Janeiro; sample 3 was investigated from room temperature up to above 900 K using a vibrating sample magnetometer (EG&G model 4500), with a maximum field of 10 kOe; samples 4 and 5 were investigated from 4.6 and 300 K using a commercial extraction magnetometer (Lake Shore model 7500) with a maximum applied field of 50 kOe. Finally, samples 6–8 were measured in Campinas from 2 to 340 K using a superconducting quantum interference device (SQUID) magnetometer (MPMS XL7), with a maximum applied field of 65 kOe. In all cases, hysteretic magnetization loops were obtained; the anhysteretic curves of all samples were determined at different temperatures by averaging the two loop branches; such a procedure is justified by previous measurements.[24]

## III. SUPERPARAMAGNETIC DESCRIPTION OF GRANULAR ALLOYS: DRAWBACKS

Bulk granular alloys are usually described as superparamagnetic (SP) at high temperatures on the basis of the following properties: (a) their anhysteretic magnetization curves are well described in terms of Langevin functions; (b) in some cases, the classical ''superparamagnetic'' scaling law of the reduced magnetization $M/M_S$ with $M_S(H/T)$ has been approximately observed;[25,26] at low temperatures, deviations from the $M_S(H/T)$ law in samples containing chemically homogeneous particles are usually ascribed to single-particle blocking. A number of experimental papers have been published in the last decade based upon the assumption that the particle moments are completely noninteracting.[3,6,27] In these works, the value of the average magnetic moment per particle and/or the width of the particle-size distribution has been obtained by fitting the anhysteretic magnetization by a superposition of Langevin functions with proper weights (in some cases, the particle-size distribution is assumed *a priori* to follow a log-normal behavior[3]). The agreement between experimental $M(H)$ curves and fitting functions is always excellent; such a circumstance has supported the simplified view of these systems as an assembly of noninteracting moments. However, some major drawbacks of the SP description have begun to emerge.

First, the scaling of $M/M_S$ with the ratio $M_S(H/T)$ is not generally observed even in temperature regions where single-particle blocking should be negligible. A bulk granular alloy of composition $Cu_{90}Co_{10}$ has been recently examined at temperatures higher than 300 K, but sufficiently low to ensure reversibility of the magnetic properties on coming back to RT (i.e., neither significant precipitation of new particles nor particle growth occurs).[5] As a matter of fact, all systems examined at high temperatures in this work exhibit the fol-

TABLE I. List of measured $Cu_{90}Co_{10}$ samples, indicating preparation parameters, previous thermal treatments, and investigated temperature ranges.

| Sample No. | Preparation parameters | Previous treatments | Laboratory and investigated temperature range (K) |
|---|---|---|---|
| 1 | Wheel velocity: 22 m/s<br>Temperature of the melt: 1100 °C | As quenched | Torino<br>300–480 |
| 2 | As in sample 1 | Annealed by Joule heating ($I=9$ A, $t=60$ s) | Torino<br>300–700 |
| 3 | Wheel velocity: 20 m/s<br>Temperature of the melt: 1200 °C | As quenched | Rio de Janeiro<br>290–480 |
| 4 | Wheel velocity: 30 m/s<br>Temperature of the melt: 1200 °C | As quenched | Rio de Janeiro<br>4–244 |
| 5 | Wheel velocity: 28 m/s<br>Temperature of the melt: 1200 °C | Annealed in furnace ($T=500$ °C, $t=3600$ s) | Rio de Janeiro<br>4–251 |
| 6 | Wheel velocity: 22 m/s<br>Temperature of the melt: 1200 °C | As quenched | Campinas<br>2–340 |
| 7 | As in sample 6 | Annealed by Joule heating ($I=5$ A, $t=60$ s) | Campinas<br>2–340 |
| 8 | As in sample 6 | Annealed by Joule heating ($I=5.5$ A, $t=60$ s) | Campinas<br>2–340 |

lowing common features: complete reversibility of the RT properties is found after a first measurement run up to 500 K; slight irreversible effects begin to be observed at room temperature after a measurement run up to about 700 K; measurements performed at even higher temperatures are characterized by irreversibility in the very course of the loop tracing (i.e., the loop branches are observed to cross). These last results have been disregarded in the following.

Although all $M(H)$ curves were well described by the sum of just two Langevin functions with proper weights, the ''superparamagnetic'' scaling law of $M/M_S$ with the product $M_S(H/T)$ was not observed [Fig. 1(b)]; on the contrary, $M/M_S$ was found to perfectly scale with the ratio $H/M_S$ [Fig. 1(a)]. Moreover, the average magnetic moment obtained by the fitting procedure was found to linearly *increase* with the ratio $T/M_S$. Actually, the particle moment is expected to stay almost constant at low $T$ and to *decrease* when $T$ approaches the Curie temperature $T_C$, owing to the corresponding reduction in $M_S$. For this reason, the particle moment obtained by the fitting procedure was referred to as an *apparent* moment;[5] however, no simple explanation was proposed for such a behavior. Even a random anisotropy model, recently applied to describe hysteretic features of these systems,[28] cannot be invoked to explain the origin and temperature evolution of the apparent moment.[29] Quite interestingly, very similar results were found at much lower temperatures in other Cu-Co granular ribbons by Dieny *et al.*;[25] in some cases, the reduced magnetization was found to scale with $M_S(H/T)$ only above 50 K, while below that temperature all $M/M_S$ vs $H$ curves were found to overlap—this is equivalent to a scaling law of the $H/M_S$ type, because the saturation magnetization is constant at low $T$. Such a behavior, observed also in more concentrated Cu-Co alloys over an extended temperature interval, was generically related to the effects of single-particle blocking and of random, collective interactions among particles.[25]

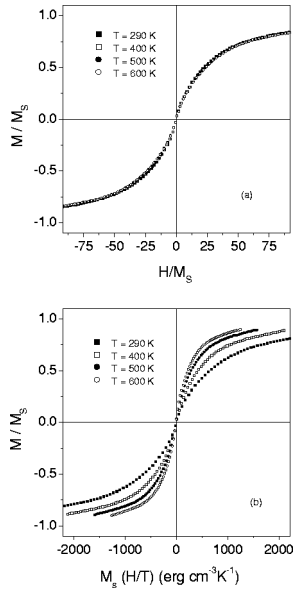


FIG. 1. Reduced magnetization of sample 2, measured at four different temperatures, and plotted as a function of $H/M_S$ (a) and $M_S(H/T)$ (b).

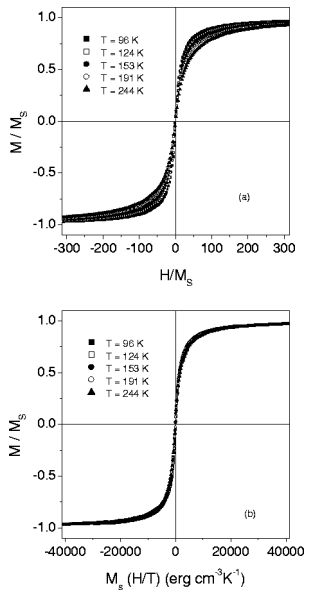


FIG. 2. Reduced magnetization of sample 5, measured at four different temperatures, and plotted as a function of $H/M_S$ (a) and $M_S(H/T)$ (b).

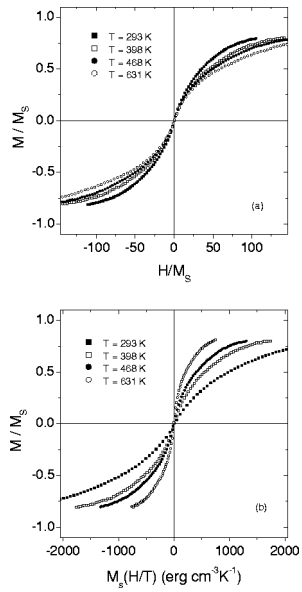


FIG. 3. Reduced magnetization of sample 3, measured at four different temperatures, and plotted as a function of $H/M_S$ (a) and $M_S(H/T)$ (b).

The puzzling behavior of the anhysteretic magnetization deserves a more systematic study. The anhysteretic $M(H)$ curves of the $Cu_{90}Co_{10}$ ribbons described in Sec. II have been submitted to a conventional fitting procedure by means of Langevin functions, so that both the saturation magnetization and the average particle moment have been determined for each temperature. The reduced magnetization is then plotted as a function either of $M_S(H/T)$ or $H/M_S$. A variety of results are obtained: sometimes, the classical ''superparamagnetic'' scaling law is followed (see an example in Fig. 2); sometimes, the curves are found to scale with $H/M_S$ (exactly as in Fig. 1); in other samples, neither the $M_S(H/T)$ nor the $H/M_S$ scaling laws are observed to hold (see an example in Fig. 3). However, in *all* examined systems (both at low and high $T$) the apparent average magnetic moment is always found to steadily *increase* with temperature (see open symbols in Figs. 4 and 5). The low-temperature limit of the apparent moment [see Figs. 4(d) and 5] is very close to zero. Undoubtedly, the intrinsic meaning of the apparent moment, as well as the adequacy of the adopted SP description, is jeopardized by these measurements.

On the other hand, the SP description can be criticized from a different point of view. Recently, numeric simulations of the effect of dipolar interactions on the magnetization and magnetoresistance of Cu-Co alloys have been published.[30–32] In spite of the limitations inherent to any numeric simulation, these data are particularly valuable because they can be obtained on model systems composed of equal Co particles having all the same magnetic moment—a condition never exactly fulfilled in real materials. There has been much debate in the past about the role of the distribution of moments on both magnetization and magnetoresistance of granular alloys.[3,31,33–37] In some model systems there is no distribution at all, and dipolar interactions may be switched on and off. According to Kechrakos and Trohidou,[31] dipolar interactions act to lower the magnetic response (susceptibility) of the system, so that $M(H)$ approaches saturation at a much slower rate than the corresponding curve for noninteracting particles. Such a behavior is reported in Fig. 6, where the data for the interacting system taken from Ref. 31 (solid symbols) are compared with the Langevin curve for the same magnetic moment ($\mu = 1.58\times10^4 \mu_B$: this is the true moment of the system) at the same temperature ($T = 82$ K). Now, the simulated curve for interacting moments is still perfectly described by a *single* Langevin function, with an *apparent* moment significantly lower than the true moment ($\mu_a = 4.0\times10^3 \mu_B$) (solid line in Fig. 6). In conclusion, the

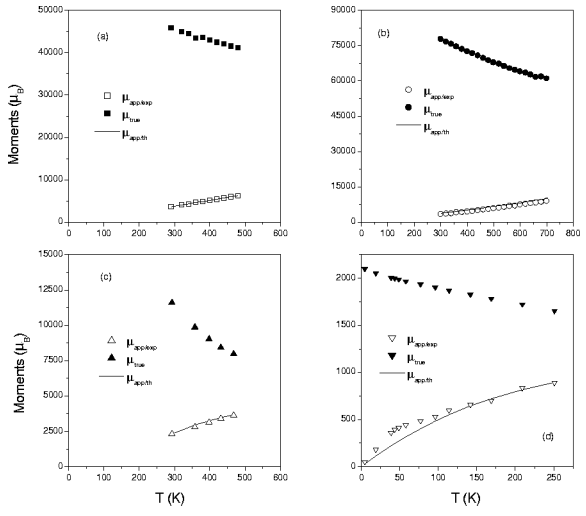


FIG. 4. Temperature behavior of apparent moments (open symbols) and true moments (solid symbols) for samples 1–4. □, sample 1; ○, sample 2; △, sample 3; ▽, sample 4. See Table II for details. Solid line: internal check of the theory [prediction of Eq. (6)].

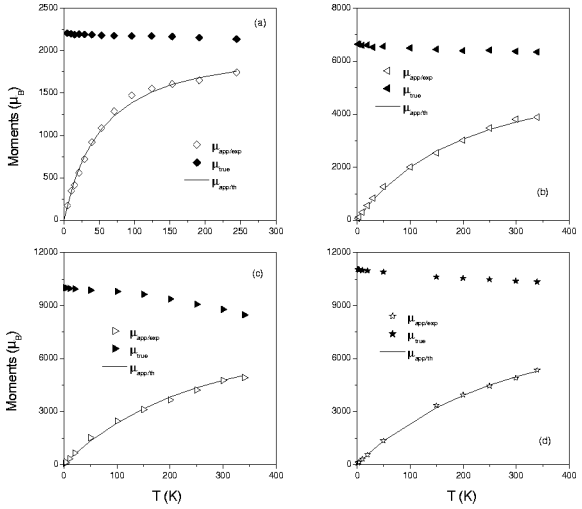


FIG. 5. The same as in Fig. 4 for samples 5–8. ◇, sample 5; ◁, sample 6; ▷, sample 7; ⋆, sample 8. See Table II for details.

magnetization curve for an assembly of identical, interacting moments can still be represented by a single Langevin function, appropriate for an assembly of identical, noninteracting moments; however, the magnetic moment and particle size estimated through this analysis are much lower than the real ones. Even more important, the presence of dipolar interactions does not emerge at all from the analysis of the $M(H)$ anhysteretic curve, leading the unaware investigator to the wrong conclusion that the system is actually composed of noninteracting particles. In our opinion, the same difficulties arise when the analysis is performed on real Cu-Co systems.

## IV. NEW MAGNETIC REGIME: THE INTERACTING SUPERPARAMAGNET

Many results, both experimental and from simulation, point to the substantial inadequacy of the SP description of granular Cu-Co alloys. Dipole-dipole interactions seem to influence the anhysteretic magnetization of these alloys; the effect of the random dipolar field acting on each dipole must be accounted for in a simplified way. This vector field, a random function of both time and space, reduces the initial rate of approach to saturation of the assembly of magnetic moments at a given temperature. It is, however, reasonable to assume that it is not sufficiently strong to overwhelm the SP features of the system; it should be rather viewed as perturbing the SP regime; as a consequence, one can attempt to introduce suitable changes in the argument of the Langevin function.

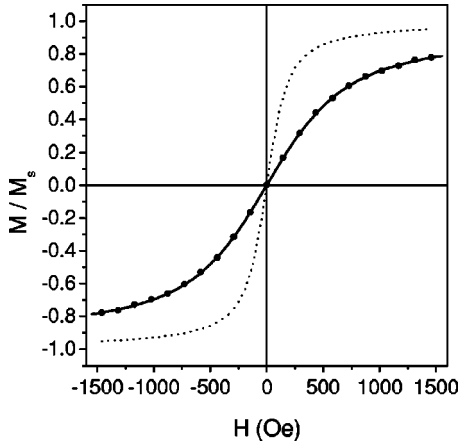


FIG. 6. Solid symbols: simulation of the anhysteretic magnetization behavior for an assembly of identical interacting Co moments ($\mu = 1.58\times10^4\mu_B$ at $T=82$ K, from Ref. 31). Dotted line: Langevin function for $\mu = 1.58\times10^4\mu_B$ at $T=82$ K. Solid line: Langevin function for $\mu = 4.0\times10^3\mu_B$ at $T=82$ K.

First, let us consider a single-moment system, i.e., a system containing magnetic particles of the same size; the extension to a distributed-moment system is straightforward and will be discussed later. The magnetization of a SP assembly of identical moments of magnitude $\mu$ is simply written as

$$M = N\mu\,\mathrm{L}\left(\frac{\mu H}{kT}\right), \tag{1}$$

where $N$ is the number of moments per unit volume and L is the Langevin function. Both $N$ and the particle size are assumed to be independent of temperature (structural changes are explicitly excluded). The results of the numerical simulations indicate that the effect of dipolar interactions may be accounted for by reducing the argument of the Langevin function in Eq. (1); this is done here by defining an apparent temperature $T_a > T$. Let us briefly justify our choice. In many topics of magnetism, the effect of collective interactions among magnetic units is accounted for by properly modifying the argument of the function which describes the magnetization of an assembly of noninteracting units. Usually these simplified theories involve an effective *field* which adds to (or subtracts from) the applied field. The experimental behavior of granular systems is clearly not described by a mean-field theory of this type; the main difference is that in most cases the collective interactions introduce an additional (either long-ranged or local) magnetic *order*, while in these granular systems the local dipolar field enhances the *disorder* of magnetic moments. As a consequence, it is more convenient to picture the effect of dipolar magnetic interactions by modifying the temperature appearing at the argument's denominator in the Langevin function. The assumption is justified considering that the dipolar field acting on any magnetic moment randomly changes in direction, sign, and magnitude at a very high rate [of the order of $1\times10^9$ Hz (Ref. 38)], exerting a disordering, random torque which opposes the ordering effect of the external magnetic field; in this sense, the role of the dipolar field may be likened to the one played by temperature and strengthens its effects. Here, the apparent temperature is simply written as $T_a = T + T^*$, where $T^*$ is not an arbitrary quantity, but is related to the rms dipolar energy $\varepsilon_D$ through the relation

$$kT^* = \varepsilon_D, \tag{2}$$

where $\varepsilon_D = \alpha\mu^2/d^3$, $d$ being the (average) interparticle distance and $\alpha$ being a proportionality constant deriving from the sum of all dipolar energy contributions;[39,40] it depends on

the actual distribution of magnetic particles in space and on the short-distance correlation possibly existing among adjacent moments; therefore, it is not obtained from first principles, although values between unity and some tens could be a reasonable estimate for this quantity. Using the condition $Nd^3=1$ and $M_S=N\mu$, the following alternative expressions of $T^*$ may be obtained:

$$T^*=\frac{\alpha}{k}\frac{\mu^2}{d^3}=\frac{\alpha}{k}N\mu^2=\frac{\alpha}{k}\frac{M_S^2}{N}. \tag{3}$$

As a consequence, it is assumed that the alloy magnetization is described by a modified Langevin function

$$M=N\mu\,\mathrm{L}\left(\frac{\mu H}{k(T+T^*)}\right), \tag{4}$$

which describes a different regime of the magnetic system, where the effect of dipolar interactions is no longer negligible. This regime will be referred to as the ''interacting superparamagnet'' (ISP). On the other hand, any experimental $M(H)$ curve fitted by Eq. (4) is also fitted by a *standard* Langevin function, where, however, an apparent moment $\mu_a$ and an apparent particle density $N_a$ must be used:

$$M=N_a\mu_a\,\mathrm{L}\left(\frac{\mu_a H}{kT}\right). \tag{5}$$

The following relations must exist between apparent and true parameters:

$$\mu_a=\frac{1}{1+\dfrac{T^*}{T}}\mu, \quad N_a=\left(1+\frac{T*}{T}\right)N. \tag{6}$$

Let us consider the magnetic regimes corresponding to the conditions $T\ll T^*$ and $T\gg T^*$. The latter is essentially coincident with the standard SP regime, so that $\mu_a\approx\mu$ and $M/M_S$ scales with $H/T$ (when $M_S$ and $\mu$ may be considered constant). On the other hand, when $T\ll T^*$ the apparent magnetic moment is much lower than the true moment and can be written as a linear function of the ratio $T/M_S$, reducing to zero for $T\to 0$:

$$\mu_a\simeq\frac{kT}{\alpha M_S}. \tag{7}$$

The reduced magnetization becomes in this regime

$$\frac{M}{M_S}\simeq\mathrm{L}\left(\frac{H}{\alpha M_S}\right). \tag{8}$$

The scaling law with respect to $H/M_S$ emerges quite naturally, $\alpha$ being a constant for a given sample. Note that in Eq. (8) the measurement temperature is no longer explicitly present in the argument of the function (an implicit dependence on $T$ occurs, however, through $M_S$).

A specific fitting procedure is now defined in order to extract the true values for $\mu$, $N$ (and $T^*$) from an experimental data set. The low-field susceptibility of the ISP system is simply

$$\chi=\frac{N\mu^2}{3k(T+T^*)}, \tag{9}$$

formally coincident with the Curie-Weiss law of a (classical) antiferromagnetic material. Indeed, an antiferromagnetic susceptibility has been experimentally observed in granular systems.[26] However, the present form of $\chi$ derives from the modified Langevin function [Eq. (4)] and does not directly imply the presence of dominant antiferromagnetic interactions in these granular systems. There are only two independent unknowns in Eq. (9): $N$ and $\alpha$ (contained in $T^*$); they can be immediately obtained plotting the inverse susceptibility against $T/M_S^2$; in such a way, after direct manipulation of Eq. (9) a linear law is derived, whose fitting parameters (slope and intercept) contain $N$ and $\alpha$, respectively:

$$\frac{1}{\chi}=3kN\left(\frac{T}{M_S^2}\right)+3\alpha. \tag{10}$$

In this way, $N$ and $\alpha$ are easily determined. Then, $\mu$ is obtained as the ratio $M_S/N$ and $T^*$ from Eq. (3). For distributed moments, a similar expression holds under more restrictive conditions. The analysis of the case of distributed moments is left to the Appendix; here, the final fitting formula is reported:

$$\frac{\rho}{\chi}=3kN\left(\frac{T}{M_S^2}\right)+3\alpha, \tag{11}$$

where $\rho$ is defined as the ratio

$$\rho=\frac{\langle\mu^2\rangle}{\langle\mu\rangle^2}\equiv\frac{\langle\mu_a^2\rangle}{\langle\mu_a\rangle^2}, \tag{12}$$

$\langle\mu\rangle$ and $\langle\mu^2\rangle$ being the average values of the particle moment and of its square. Equation (11) has been used in this work to obtain $N$ and $\alpha$ (hence $\langle\mu\rangle$ and $T^*$) for all examined Cu-Co systems. It is interesting to note that a linear dependence of the quantity $\rho/\chi$ on the ratio $T/M_S^2$ is always experimentally observed over a wide temperature range, as shown in Fig. 7 (in a single case a strong deviation from linearity occurs at low temperatures [Fig. 7(b)]; such a behavior is possibly related to particularly strong spurious effects, such as single-particle blocking). The best-fit values of $N$, $\alpha$, $T^*(300\ \mathrm{K})$, and $\langle\mu\rangle$ (300 K) are reported in Table II, together with the equivalent particle radius $\langle R\rangle$ obtained by assuming spherical particles and taking $M_S^{Co}=1400\ \mathrm{emu/cm^3}$ at room temperature. The temperature behavior of the true average moment $\langle\mu\rangle$ is reported in Figs. 4 and 5; it merely reflects the experimental decrease of $M_S$. Values of $\langle\mu\rangle$ substantially larger than $\langle\mu_a\rangle$ are found in certain cases; this means that the particle sizes estimated by fitting the experimental $M(H)$ curves to standard Langevin functions are always lower than the real ones. An internal

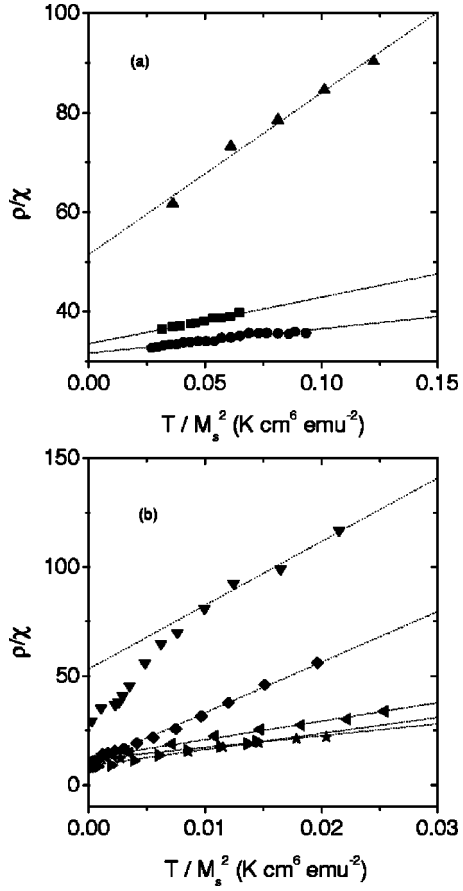


FIG. 7. Experimental plots of the quantity $\rho/\chi$ vs $T/M_S^2$ [Eq. (11)] for all examined $Cu_{90}Co_{10}$ samples. Samples identified as in Figs. 4 and 5.

check of the theory may be done comparing the $\langle \mu_a \rangle$ results obtained through the SP fitting procedure (open symbols in Figs. 4 and 5) with the predictions of the present theory, estimated using the $\langle \mu \rangle$ data and Eq. (6) (solid lines in Figs. 4 and 5); the agreement is always excellent.

The values of $T^*$ obtained by this procedure appear to strongly vary from sample to sample (see Table II). In fact, using Eq. (3), $T^*$ can be cast into the form

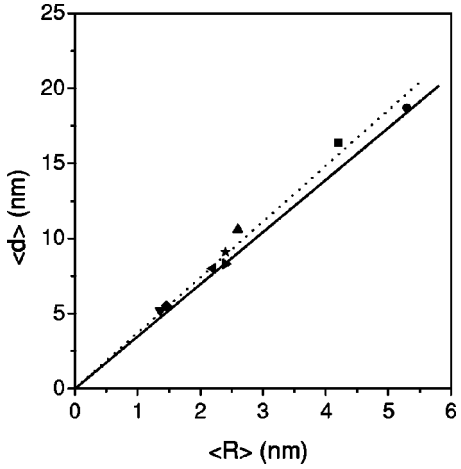


FIG. 8. Symbols: average interparticle distance vs equivalent particle radius for samples 1 to 8 (identified as in Figs. 4 and 5). Solid line: ideal prediction for $Cu_{90}Co_{10}$. Dotted line: best-fit line, corresponding to the composition $Cu_{91.8}Co_{8.2}$.

$$T^* = \frac{\alpha}{k}[M_S^{FM}]^2 \langle v \rangle, \tag{13}$$

where the relations $\langle \mu \rangle = M_S^{FM} \langle v \rangle$ and $\langle d \rangle^3 = \langle v \rangle / x$ hold, $\langle v \rangle$ is the average particle volume, and $x$ is the fraction of the ferromagnetic metal (FM) atoms present in the form of particles ($0 \leqslant x \leqslant 1$). Equation (13) shows that $T^*$ at a given temperature and for a given ferromagnetic metal increases with both $x$ and $\langle v \rangle$. Having determined the true particle sizes and densities, it is possible to draw on a firmer basis some conclusions about the granular structure of the examined samples. The relationship between average interparticle distance $\langle d \rangle$ and average particle radius $\langle R \rangle$ is shown in Fig. 8. The data are linearly correlated, according to the relation

$$\langle d \rangle = \left( \frac{4\pi}{3x} \right)^{1/3} \langle R \rangle, \tag{14}$$

obtained using $\langle d \rangle^3 = \langle v \rangle / x$ and assuming that the particles are spherical. The straight line obtained from Eq. (14) with $x = 0.1$ is shown in Fig. 8 (solid line). The best-fit line through the data has a slightly higher slope, corresponding to

TABLE II. Best-fit values of $N$ and $\alpha$ obtained through Eq. (11) for all studied $Cu_{90}Co_{10}$ samples. The resulting interaction temperature, average magnetic moment, and equivalent particle radius are also reported.

| Alloy | $N(\mathrm{cm}^{-3})$ | $\alpha$ | $T^*$ [300 K] | $\langle \mu \rangle$ [300 K] ($\mu_B$) | $\langle R \rangle$ (nm) |
|---|---|---|---|---|---|
| 1 | $2.26\times10^{17}$ | 11.2 | 3310 | $4.59\times10^{4}$ | 4.2 |
| 2 | $1.53\times10^{17}$ | 10.4 | 5960 | $7.78\times10^{4}$ | 5.3 |
| 3 | $8.38\times10^{17}$ | 16.7 | 1170 | $1.16\times10^{4}$ | 2.6 |
| 4 | $7.05\times10^{18}$ | 17.8 | 210[a] | $8.93\times10^{2}$[a] | 1.4 |
| 5 | $6.08\times10^{18}$ | 2.4 | 55[b] | $2.14\times10^{3}$[b] | 1.5 |
| 6 | $1.97\times10^{18}$ | 4.3 | 215 | $6.37\times10^{3}$ | 2.2 |
| 7 | $1.77\times10^{18}$ | 3.0 | 270 | $8.77\times10^{3}$ | 2.4 |
| 8 | $1.34\times10^{18}$ | 3.6 | 325 | $1.04\times10^{4}$ | 2.4 |

[a]At $T = 251$ K.
[b]At $T = 244$ K.

$x=0.082$. This means that, generally speaking, a fraction of Co atoms are still dissolved in the Cu matrix. Some experimental points fall very close to the solid line; no experimental points fall *below* it.

The present theory implies that particle sizes determined from the conventional analysis of magnetization curves are systematically underestimated. It would be useful to have this prediction supported by structural data obtained from direct observation. Quite unfortunately, in Cu-Co alloys the Co-cluster size is hardly determined by x-ray diffraction (XRD) and tunneling electron microscopy (TEM) because of the high coherency of Co and Cu lattices and of the comparatively small lattice mismatch. As a consequence, few structural results on the Cu-Co system are available in the literature; the particle size as determined by structural investigations is always in qualitative agreement with the value obtained from magnetic measurements on similar materials.[25,41–43] More interesting to the present discussion would be a direct comparison between magnetic and structural data taken on the same alloy. In the case of the Cu-Co system and, to our knowledge, a single explicit attempt to compare the Co-particle size obtained in a $Cu_{80}Co_{20}$ alloy from magnetic and structural measurements exists:[27] X-ray diffraction provides a slightly larger value than magnetic analysis does; a recent paper[44] deals with magnetic and structural measurements in superparamagnetic $Fe_{63.5}Cr_{10}Si_{13.5}B_9Cu_1Nb_3$ (well above the Curie temperature of the amorphous intergranular phase): even in this case, the particle size as determined by x-ray diffraction is higher than the one deduced from the $M(H)$ curves. Both results are in good qualitative agreement with the predictions of the present model.

## V. MAGNETIC-REGIME DIAGRAM

The proposed approach is appropriate to describe the temperature behavior of the *apparent* moments and of the low-field susceptibility of Cu-Co systems. Remarkably, the apparent moments are well reproduced by the ISP model down to very low temperatures, where the conventional SP model is known to lose validity by effect of particle blocking. Only in a single case [Fig. 7(d)] has a substantial deviation between experimental results and theory been observed at low $T$ [the same lack of consistency was already noticed in the $\rho/\chi$ vs $T/M_S^2$ plot in Fig. 7(b)]. Equation (4) seems to be suitable to describe the anhysteretic behavior of granular systems over an extended temperature interval. Of course, single-particle blocking must occur at sufficiently low temperatures; on the other hand, when dipolar interactions among particles are present, different low-$T$ blocking mechanisms should be explicitly considered, such as collective blocking of moments. Having introduced the temperature $T^*$ as a suitable parameter to describe the dipolar interactions, some simple consequences can be immediately drawn, allowing us to propose a magnetic-regime diagram. Let us first introduce the following three critical volumes for particles.

(a) The single-particle blocking volume $v_{B_S}$, defined as usual as

$$v_{B_S}=\frac{k}{K_A}\ln\left(\frac{\tau_m}{\tau_0}\right)T, \tag{15}$$

where $\tau_m$ is the measurement time, $\tau_0^{-1}$ is the attempt frequency for particle magnetization reversal, and $K_A$ is the anisotropy energy constant; $v_{B_S}$ diverges as $T$ approaches $T_C$ because $K_A\rightarrow 0$; the value of $\ln(\tau_m/\tau_0)$ is usually taken equal to 25.[39,45]

(b) The SP-ISP boundary volume $v_{ISP}$, defined at each temperature as the particle volume for which $T^*$ equals $T$. Requiring that $T^*=T$ and using Eq. (3) one gets

$$v_{ISP}=\frac{kx}{\alpha}\left(\frac{T}{M_S^2}\right). \tag{16}$$

At each temperature, the system behaves as an interacting superparamagnet when $\langle v\rangle > v_{ISP}$ and as a standard SP when $\langle v\rangle < v_{ISP}$; $v_{ISP}$ diverges as $T$ approaches $T_C$ owing to the $M_S^{-2}$ factor.

(c) The collective blocking volume $v_{B_C}$, defined at each temperature as the particle volume for which the time needed by the system of moments to overcome the energy barrier for collective blocking, $\varepsilon_D$, equals the measurement time $\tau_m$; specifically,

$$\tau_m=\tau_0' e^{\varepsilon_D/kT}=\tau_0' e^{T^*/T}, \tag{17}$$

where $\tau_0'$ is a preexponential constant. Using Eq. (3) one gets

$$v_{B_C}=\frac{kx}{\alpha}\ln\left(\frac{\tau_m}{\tau_0'}\right)\left(\frac{T}{M_S^2}\right). \tag{18}$$

At each temperature, the system undergoes collective blocking when $\langle v\rangle > v_{B_C}$; it behaves as an interacting SP when $\langle v\rangle < v_{B_C}$; $v_{B_C}$ diverges as $T$ approaches $T_C$ owing to the $M_S^{-2}$ factor.

Using appropriate parameter values and assuming $\tau_0 \approx \tau_0' \approx 10^{-9}$ s and $\tau_m \approx 10^2$ s,[39,45] it is possible to draw a magnetic-regime diagram for each granular system. Two examples are shown in Fig. 9; the upper diagram refers to the highly idealized case of spherical fcc Co particles whose magnetization and anisotropy energy follow those of pure bulk Co in the fcc phase. For any particle radius, on continuously lowering the temperature below $T_C$, the particle moments first behave superparamagnetically; then the ISP regime emerges; then *collective* particle blocking ($B_C$) occurs. Single-particle blocking ($B_S$) would appear at even lower temperatures. The lower diagram of Fig. 9 refers to one of the real Cu-Co systems examined in this paper (sample 6; the experimental $\langle R\rangle$ value is reported in the figure). Although the boundary lines between regimes are displaced with respect to the upper diagram, the same sequence SP$\rightarrow$ISP $\rightarrow B_C$ is found. Qualitatively similar results are obtained in all other systems. Again, single-particle blocking would occur at temperatures lower than collective blocking. It should, however, be noted that in the case of distributed particle radii, the $v_{B_S}$ line defines the blocking of particles with ra-

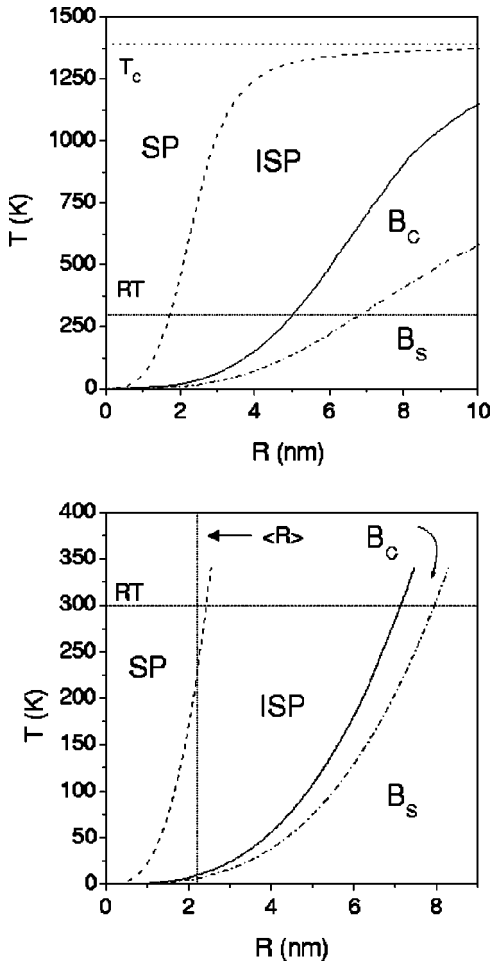


FIG. 9. Magnetic regime diagrams for ideal fcc Co particles (composition: $Cu_{90}Co_{10}$) with magnetization and anisotropy values of bulk Co (a) and for a real $Cu_{90}Co_{10}$ alloy (sample 6) (b). SP, superparamagnet; ISP, interacting superparamagnet; $B_C$, collective blocked regime; $B_S$, single-particle blocked regime. $\langle R \rangle$ in diagram (b) is the experimentally determined equivalent radius for sample 6.

dius equal to the average radius; single-particle blocking of larger particles would occur at higher temperatures.

Two further comments on these diagrams are appropriate: (a) the reported boundary lines should not be intended as separating different phases in a thermodynamic sense; they merely help to individuate ''fuzzy'' transitions between different regimes, slowly transforming from one to the other with decreasing $T$; this is particularly true for the SP-ISP boundary line; (b) a competition between collective and single-particle blocking always emerges; our data seem to indicate that collective blocking is favored, in agreement with indications from zero-field-cooled (ZFC) and field-cooled (FC) susceptibility curve analysis.[46] This fact could explain why Eq. (4) is suitable to describe the $M(H)$ curve down to low temperatures.

A major role in the theory is played by the ratio $T^*/T$. The value $T^*/T=1$ conventionally corresponds to the transition between SP and ISP regimes, while $T^*/T=25$ marks the transition between ISP and (collectively) blocked regimes. The quantity $T^*/T$, obtained from Eq. (3) using the values of $N$ and $\alpha$ reported in Table II, is plotted in Fig. 10 as a function of $T$ for all considered Cu-Co systems (the samples are identified by the same symbols as in previous figures). The region between the horizontal parallel lines corresponds to the ISP regime. In one case many representative points fall well within the SP regime at high temperature (sample 5); in fact, the reduced magnetization of this sample scales with $M_S(H/T)$ (Fig. 2); on the contrary, a scaling law of the $H/M_S$ type is observed for the reduced magnetization of alloys whose representative points fall in the upper ISP or blocked regimes (Fig. 1); the reduced magnetization of an alloy with representative points in the lower ISP regime (open triangles) scales neither with $M_S(H/T)$ nor with $H/M_S$ (Fig. 3). Some of the representative point sets extend from the ISP-SP boundary up to the blocked region; in all these cases, the reduced magnetization scales with $M_S(H/T)$ at higher temperatures and with $H/M_S$ at lower temperatures, changing from one regime to the other in a continuous way. In our opinion, this is a most convincing proof of the adequacy of the present approach.

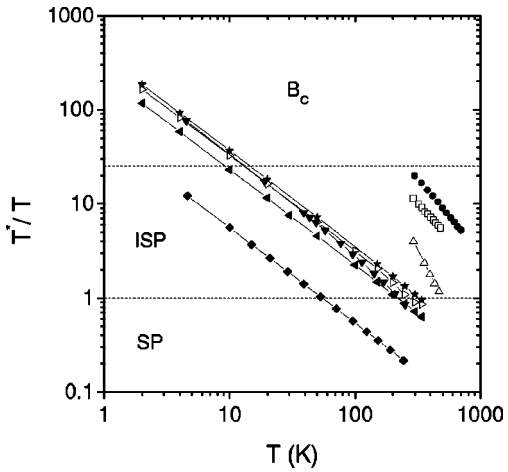


FIG. 10. Behavior of the ratio $T^*/T$ as a function of $T$ for samples 1–8 identified as in Figs. 4 and 5. $B_C$, collective blocked regime; ISP, interacting superparamagnet; SP, superparamagnet.

Finally, it can be interesting to compare the collective blocking temperatures as obtained for all materials from Fig. 10 to the single-particle blocking temperatures calculated using Eq. (15). To this aim, however, some simplifying assumptions must be made: (a) perfectly spherical particles are assumed, (b) the particle volume is taken equal to the average value obtained from the radius appearing in Table I, and (c) the dominant anisotropy constant is assumed to be that of fcc Co particles, following the temperature behavior reported in the literature for fcc Co (Ref. 47) and matching the value given in Ref. 42 ($K_A=2.310^5$ erg/cm$^3$ at 773 K). Of course, different results would be obtained assuming, e.g., nonspherical particles. The temperatures obtained for single-particle blocking ($T_{B_S}$) are listed in Table III along with the corresponding values for $T_{B_C}$ taken from Fig. 10. All single-blocking temperatures lie below the corresponding temperatures of collective blocking, although in some cases this regime occurs only in a narrow temperature interval. In conclusion, a real competition between the two blocking re-

TABLE III. Collective blocking and single-particle blocking temperature for all the examined systems.

| Alloy | $T_{B_C}$ (K) | $T_{B_S}$ (K) |
|---|---|---|
| 1 | 160 | 42 |
| 2 | 260 | 80 |
| 3 | 145 | 11 |
| 4 | 13 | 4.2 |
| 5 | 2.5 | 4.5 |
| 6 | 9 | 6.5 |
| 7 | 13 | 8.5 |
| 8 | 15 | 8.5 |

gimes may occur in some cases (small particle sizes); in other samples, collective blocking effects seem to be predominant.

## VI. CONCLUDING REMARKS

The procedure described in Sec. IV allows one to obtain the ''true'' average magnetic moment and the ''true'' particle density of a granular magnetic system. These quantities often significantly differ from the ''apparent'' values obtained using the naive superparamagnetic description.

The picture emerging from the analysis seems to be apt to interpret many puzzling aspects of the magnetic properties of all examined granular systems. In our opinion, the physical concepts developed in this paper are rather general, so that they are not necessarily limited to a single composition or a single alloy family such as $Cu_{100-x}Co_x$; they should instead be extended to other bulk granular systems or granular films of the type FM-(Met), where FM is any ferromagnetic metal and (Met) is a nonmagnetic metal, and more generally to systems where particles of a ferromagnetic material are embedded in any nonmagnetic matrix. A systematic study of granular magnetic systems differing by the type of magnetic particles and host material, by their concentration, or by sample dimensionality is, however, still to be performed.

The proposed model explains coherently and in a simple way a variety of seemingly inconsistent magnetic results, providing at the same time a new view of the magnetic regimes of an interesting class of magnetic systems. It therefore marks a remarkable step forward with respect to the simple superparamagnetic description adopted so far. Moreover, it has further potential applications: for instance, let us explicitly note that Eq. (9) or (A5) should allow one to exploit the information obtained from the anhysteretic magnetization in order to predict the form of ZFC susceptibility curves.

However, the model has unavoidable, intrinsic limits: in particular, it must be merely regarded as a suitable *description* of a (nontrivial) magnetic behavior, i.e., as an interpretative scheme rather than a complete theory. A number of fundamental questions remain unanswered.

The core of the model is Eq. (4) [or its equivalent for distributed moments, Eq. (A1)]. There, the complex, collective effects of dipolar interactions are taken into account in a mostly simplified, but particularly effective way.

Let us briefly comment on the problems inherent to the form of Eqs. (4) and (A1), considering first the higher-temperature limit, i.e., the ISP regime. A first puzzling aspect emerges: the ''interaction'' temperature $T^*$ may be much larger than the measurement temperature, and the parameter $\alpha$ may assume rather high values, as observed in Table II. The variety of $\alpha$ values resulting from our best-fit procedure could reflect not only changes in the spatial distribution of particles or in their degree of correlation, but also the presence of additional interactions among particles. Indeed, long-ranged, indirect interactions of RKKY type, often assumed to play a role in granular metallic systems,[48] are still proportional to the ratio $\mu^2/d^3$ and could contribute as well to the interaction temperature $T^*$. Of course, when $T$ is increased towards $T_C$, $T^*$ rapidly drops, to finally vanish for $T = T_C$. This means that for sufficiently high temperatures, any granular alloy can be described as a *bona fide* superparamagnet (see Fig. 9). On cooling, the effect of $T^*$ becomes stronger, to finally become dominant. A question immediately arises about the interactions, which are sufficiently strong to substantially modify the argument of the Langevin function, but do not change the functional form of the $M(H)$ curve. As a matter of fact, the shape of the experimental $M(H)$ curves of granular systems does not exhibit any trace of an abrupt change to another functional dependence when the temperature is lowered: the anhysteretic curves retain their Langevin-like features, and each one can be obtained from another just by changing the argument of the Langevin function; moreover, the hysteresis loops maintain a shape not much differing from the one measured at high $T$ and well described by the interacting-particle model.[6] Incidentally, these anhysteretic and hysteretic characters are typically not reproduced by computer simulations where local anisotropies and single-particle blocking processes are assumed to play a dominant role.[49,32] Such a circumstance, occurring in many granular systems, contributes to support the hypothesis that any description involving a modified Langevin function is appropriate.

Even more complex problems arise when the temperature is so much lowered that a blocked regime occurs. In this case, the moments are expected to be frozen in random directions; no *dynamic* disorder is provided by interactions. The previous picture of an enhancement of thermal disorder is therefore no longer valid in the blocked regime. Nevertheless, Eq. (4) or (A1) still adequately describes the experimental $M(H)$ curves.

Obviously, the aim of providing definite answers to such fundamental problems falls far beyond the limits and scope of a heuristic approach such as the present one. However, the indisputable ability of Eqs. (4) and (A1) to describe the anhysteretic magnetization of magnetic granular systems suggests that any more fundamental theory should lead to an equivalent final formula.

## ACKNOWLEDGMENTS

This work has been supported by INFM–PRA ELTMAG. Two of the authors acknowledge the financial

support given by some Brazilian research agencies (M.K.: CNPq, FAPESP; M.A.N.: CNPq, FUJB, and FAPERJ).

## APPENDIX

Let us make use of a discretized formalism. The distributed moments on particles $\mu_i$ $(i=1,2,\ldots,n)$ appear with probability $p_i$. The ISP magnetization is

$$M = N\sum_i p_i \mu_i \mathrm{L}\left(\frac{\mu_i H}{k(T+T^*)}\right), \tag{A1}$$

where $T^* = \alpha\langle\mu\rangle^2/\langle d\rangle^3$, $\langle\mu\rangle$ being the average moment, related to $M_S$ by the relation $M_S = N\langle\mu\rangle$, and $\langle d\rangle$ is the average interparticle distance. The magnetization can also be reproduced by a superposition of standard Langevin functions, introducing a set of apparent moments $\mu_{ai}$:

$$M = N_a\sum_i p_i \mu_{ai} \mathrm{L}\left(\frac{\mu_{ai} H}{kT}\right). \tag{A2}$$

Let us suppose that the $M(H)$ curve is described by Eq. (A2) with apparent moments weighted with the *same* probabilities $p_i$ of the true moments appearing in Eq. (A1). No doubt this is a restrictive hypothesis, justified only by simplicity reasons. The assumption that the $p_i$'s are the same for the distributions of true and apparent moments allows one to use the standard fitting procedure through Eq. (A2) to obtain the form of the moment distribution function. Under this hypothesis, the following relation univocally relates each apparent moment to a true moment:

$$\mu_{ai} = \frac{1}{1+\dfrac{T^*}{T}}\mu_i, \tag{A3}$$

so that a similar relation holds for the average values,

$$\langle\mu_a\rangle = \frac{1}{1+\dfrac{T^*}{T}}\langle\mu\rangle. \tag{A4}$$

The low-field susceptibility is now

$$\chi = \frac{M\sum_i p_i\mu_i^2}{3k(T+T^*)} = \frac{N\langle\mu^2\rangle}{3k(T+T^*)}. \tag{A5}$$

Defining the parameter ratio $\rho$ (a pure number) as

$$\rho = \frac{\langle\mu^2\rangle}{\langle\mu\rangle^2} \tag{A6}$$

and using $M_S = N\langle\mu\rangle$, Eq. (11) of Sec. IV is derived in a straightforward way. Obviously, when the distribution function is $\delta$ like, $\rho=1$, and Eq. (11) reduces to Eq. (10). If the $p_i$s are the same for both true and apparent moments, Eq. (A3) implies that

$$\frac{\langle\mu_a^2\rangle}{\langle\mu_a\rangle^2} = \frac{\langle\mu^2\rangle}{\langle\mu\rangle^2} \equiv \rho, \tag{A7}$$

so that the parameter $\rho$ can be obtained from a standard fitting procedure through Eq. (A2), i.e., *before* the evaluation of true moments, and can be used in Eq. (11) to this aim.


[1] See, for example, *Nanomagnetism*, Vol. 247 of *NATO Advanced Study Institute, Series E: Applied Sciences*, edited by A. Hernando (Plenum, New York, 1993).

[2] See, for example, Proceedings of the Magnetism of Nanostructured Phases, MNP Conference, San Sebastian, Spain, 1998, edited by J. Gonzales [J. Magn. Magn. Mater. **203** (1999)].

[3] E. F. Ferrari, F. C. S. da Silva, and M. Knobel, Phys. Rev. B **56**, 6086 (1997).

[4] A. E. Berkowitz, J. R. Mitchell, M. J. Carey, A. P. Young, S. Zhang, F. E. Spada, F. T. Parker, A. Hütten, and G. Thomas, Phys. Rev. Lett. **68**, 3745 (1992); J. Q. Xiao, J. S. Jiang, and C. L. Chien, *ibid.* **68**, 3749 (1992).

[5] P. Allia, M. Coisson, P. Tiberto, and F. Vinai, J. Magn. Magn. Mater. (to be published).

[6] P. Allia, M. Coisson, M. Knobel, P. Tiberto, and F. Vinai, Phys. Rev. B **60**, 12 207 (1999).

[7] R. Iglesias, H. Rubio, and S. Suarez, Appl. Phys. Lett. **73**, 2503 (1998).

[8] A. J. Rondinone, A. C. S. Samia, and Z. J. Zhang, Appl. Phys. Lett. **76**, 3624 (2000).

[9] R. W. Chantrell, N. Walmsley, J. Gore, and M. Maylin, Phys. Rev. B **63**, 024410 (2001).

[10] M. F. Hansen, C. B. Koch, and S. Morup, Phys. Rev. B **62**, 1124 (2000).

[11] J. F. Loffler, H. B. Braun, and W. Wagner, Phys. Rev. Lett. **85**, 1990 (2000).

[12] S. I. Denisov, V. F. Nefedchenko, and K. N. Trohidou, J. Phys.: Condens. Matter **12**, 7111 (2000).

[13] R. Prozorov, Y. Yeshurun, T. Prozorov, and A. Gedanken, Phys. Rev. B **59**, 6956 (1999).

[14] H. D. Pfannes, A. Mijovilovich, R. Magalhaes-Paniago, and R. Paniago, Phys. Rev. B **62**, 3372 (2000).

[15] B. Idzikowski, U. K. Roler, D. Eckert, K. Nenkov, and K.-H. Muller, Europhys. Lett. **45**, 714 (1999).

[16] M. Respaud, J. Appl. Phys. **86**, 556 (1999).

[17] P. J. Gregg and L. Bessais, J. Magn. Magn. Mater. **202**, 554 (1999).

[18] C. S. Martins and F. P. Missell, J. Magn. Magn. Mater. **205**, 275 (1999).

[19] J. L. Dormann, D. Fiorani, and E. Tronc, Adv. Chem. Phys. **98**, 283 (1997).

[20] S. Morup, Europhys. Lett. **28**, 671 (1994).
[21] T. Jonsson, P. Svedlindh, and M. F. Hansen, Phys. Rev. Lett. **81**, 3976 (1998).
[22] P. Allia, M. Knobel, P. Tiberto, and F. Vinai, Phys. Rev. B **52**, 15 398 (1995).
[23] P. Allia, M. Baricco, P. Tiberto, and F. Vinai, Rev. Sci. Instrum. **64**, 1053 (1993).
[24] P. Allia, M. Coisson, P. Tiberto, and F. Vinai, Nanostruct. Mater. **11**, 757 (1999).
[25] B. Dieny, A. Chamberod, C. Cowache, J. B. Genin, S. R. Teixeira, R. Ferre, and B. Barbara, J. Magn. Magn. Mater. **135**, 191 (1994).
[26] A. Gonzales, P. Tiberto, A. Garcia-Escorial, J. P. Sinnecker, P. Allia, and A. Hernando, J. Phys. IV **8**, 343 (1998).
[27] R. H. Yu, X. X. Zhang, J. Tejada, M. Knobel, P. Tiberto, and P. Allia, J. Appl. Phys. **78**, 392 (1995).
[28] W. C. Nunes, M. A. Novak, M. Knobel, and A. Hernando, J. Magn. Magn. Mater. (to be published).
[29] An apparent moment increasing with temperature is indeed compatible, at least in principle, with the interparticle correlation, as admitted by the random anisotropy model. In the presence of dominant antiferromagnetic correlation, the ordering magnetic units, built up of a number of neighboring correlated particles, could be characterized by a total (apparent) moment smaller than the sum of the individual moments on the constituent particles. Such a magnetic correlation would be destroyed by both temperature and applied field: the first effect would lead to an increase of the apparent moment value with increasing $T$ (as observed); the second effect is required to justify the experimental finding that all particle moments become aligned at sufficiently high fields. However, it is possible to show that in this case the isothermal curves of anhysteretic magnetization, affected by the progressive loss of local antiferromagnetic correlation, would definitely lose their Langevin-like characters, in sharp contrast with measurements. As a consequence, such an interpretation has to be rejected.
[30] M. El-Hilo, R. W. Chantrell, and K. O'Grady, J. Appl. Phys. **84**, 5114 (1998).
[31] D. Kechrakos and K. N. Trohidou, Phys. Rev. B **62**, 3941 (2000).
[32] A. D. Liu and H. N. Bertram, J. Appl. Phys. **89**, 2861 (2001).
[33] Jianbiao Dai and Jinke Tang, Appl. Phys. Lett. **76**, 3968 (2000).
[34] L. Sheng, H. Y. Teng, and D. Y. Xing, Phys. Rev. B **58**, 6428 (1998).
[35] Y. G. Pogorelov, M. M. P. de Azevedo, and J. B. Sousa, Phys. Rev. B **58**, 425 (1999).
[36] H. K. Lachowicz, A. Sienkiewicz, P. Gierlowski, and A. Slawska-Waniewska, J. Appl. Phys. **88**, 368 (2000).
[37] A. Garcia Prieto, M. L. Fdez-Gubieda, A. Garcia-Arribas, J. M. Barandiaran, C. Meneghini, and S. Mobilio, J. Magn. Magn. Mater. **221**, 80 (2000).
[38] P. Allia, P. Tiberto, and F. Vinai, J. Appl. Phys. **81**, 4599 (1997).
[39] A. H. Morrish, *The Physical Principles of Magnetism* (Wiley, New York, 1966).
[40] C. Kittel, *Introduction to Solid State Physics* (Wiley, New York, 1968).
[41] R. Busch, F. Grtner, C. Borchers, P. Haasen, and R. Bormann, Acta Metall. Mater. **43**, 3467 (1995).
[42] A. Htten and G. Thomas, Ultramicroscopy **52**, 581 (1993).
[43] R. Hattenhauer and P. Haasen, Philos. Mag. A **68**, 1195 (1993).
[44] V. Franco, C. F. Conde, A. Conde, L. F. Kiss, D. Kapts, T. Kemny, and I. Vincze, J. Appl. Phys. **90**, 1558 (2001).
[45] B. D. Cullity, *Introduction to Magnetic Materials* (Addison-Wesley, Reading, MA, 1972).
[46] D. Fiorani, A. M. Testa, E. Agostinelli, P. Imperatori, R. Caciuffo, D. Rinaldi, P. Tiberto, F. Vinai, and P. Allia, J. Magn. Magn. Mater. **202**, 123 (1999).
[47] *Magnetic Properties of Metals*, edited by H. P. J. Wijn, Landolt-Börnstein, New Series, Group III, Vol. 19, Pt. a (Springer-Verlag, Berlin, 1986), p. 45.
[48] D. Altbir, J. d'Albuquerque de Castro, and P. Vargas, Phys. Rev. B **54**, R6823 (1996).
[49] C. Xu, Z. Y. Li, and P. M. Hui, J. Appl. Phys. **89**, 3403 (2001).